

Article

Aeration Biofilter Filler Screening and Experimental Research on Nitrogen and Phosphorus Purification in Rural Black Water

Peizhen Chen [†] , Dongkai Chen [†], Wenjie Zhao and Xiangqun Zheng ^{*}

Agro-Environmental Protection Institute, Ministry of Agriculture and Rural Affairs, Tianjin 300191, China; chenpeizhencpz@sina.com (P.C.); chendongkai2020@126.com (D.C.); zwj1997jc@163.com (W.Z.)

^{*} Correspondence: zhengxiangqun@aepi.org.cn

[†] These authors contributed equally to this work.

Abstract: In rural toilets, black water still remains polluted by nitrogen and phosphorus after being pre-treated by septic tanks. This study uses aerated biofilters to purify black water, screen the biofilter filler, and determine its effect on nitrogen and phosphorus purification in rural black water. This study introduced the concept of the “shape factor” into the Langmuir and Freundlich equations and optimized the isotherm adsorption model to better fit the actual dynamics of nitrogen and purification in black water. Combined with the first-order kinetic equation, the double constant equation, and the Elovich equation, the adsorption performance of seven kinds of biofilter fillers (i.e., zeolite, volcanic rock, sepiolite, ceramsite, anthracite, vermiculite, and peat) was studied. Then, the biofilter was constructed using a combination of fillers with better adsorption properties, and its ability to purify rural black water was studied. Results showed that vermiculite and zeolite had little effect on nitrogen and a high saturated adsorption of 654.50 and 300.89 mg·kg⁻¹, respectively; peat and ceramsite had little effect on phosphorus and a high saturated adsorption of 282.41 mg·kg⁻¹ and 233.89 mg·kg⁻¹, respectively. The adsorption rate of nitrogen from fast to slow was vermiculite > peat > zeolite > volcanic rock > sepiolite > ceramsite > anthracite. The adsorption rate of phosphorus from fast to slow was peat > ceramsite > zeolite > sepiolite > vermiculite > volcanic rock > anthracite. Four combined biological filter fillers aided the removal of nitrogen and phosphorus from rural high-concentration black water. The combination of zeolite and ceramsite filler had a good nitrogen and phosphorus removal effect in high-concentration black water. After the system was stable, the nitrogen removal rate attained 71–73%, and the phosphorus removal rate attained 73–76% under the influent condition of total nitrogen and phosphorus concentrations of 150–162 and 10–14 mg·L⁻¹, respectively. This study provides technical support and reference for the purification and treatment of rural black water.



Citation: Chen, P.; Chen, D.; Zhao, W.; Zheng, X. Aeration Biofilter Filler Screening and Experimental Research on Nitrogen and Phosphorus Purification in Rural Black Water. *Water* **2022**, *14*, 957. <https://doi.org/10.3390/w14060957>

Academic Editors: Stefano Papirio and Carmen Teodosiu

Received: 5 February 2022

Accepted: 15 March 2022

Published: 18 March 2022

Publisher's Note: MDPI stays neutral with regard to jurisdictional claims in published maps and institutional affiliations.



Copyright: © 2022 by the authors. Licensee MDPI, Basel, Switzerland. This article is an open access article distributed under the terms and conditions of the Creative Commons Attribution (CC BY) license (<https://creativecommons.org/licenses/by/4.0/>).

Keywords: biofilter; form factor; filler; nitrogen; phosphorus

1. Introduction

Blackwater refers to toilet fecal sewage, including human urine, feces, and sewage from toilet flushing [1]. Blackwater is a major part of the domestic sewage. Approximately 1.4 billion people in China, and 800 million farmers live in rural areas. The annual production of domestic sewage in rural China is estimated to exceed 9 billion tons, and the annual output of human excrement and urine reaches 260 million tons, most of which have not been safely disposed of. The problem of toilet manure pollution control in a rural living environment cannot be ignored. It is directly related to the residents' health and environmental conditions [2]. The pollutant components in blackwater account for a very high proportion of the total load of domestic sewage pollution. TN (total nitrogen), NH₄⁺-N (ammonia nitrogen), and TP (total phosphorus) account for >84%, and are the main components of pollutants [3]. The septic tank connected to the toilet can effectively decompose the organic matter in blackwater through long-term anaerobic fermentation [4]. However, the septic tank effluent still contains high nitrogen and phosphorus concentrations due to insufficient nitrogen and phosphorus removal conditions. A direct discharge

will cause not only large non-point source pollution, water eutrophication, and biological hypoxia, but also affect human health [5,6]. Therefore, in China, where the rural population accounts for a large proportion, research on nitrogen and phosphorus purification in rural blackwater is highly significant.

Presently, the secondary treatment of effluent from rural septic tanks is mostly based on soil infiltration, constructed wetlands, and other land treatment technologies [7,8]. Although the land treatment system can achieve a certain effect, it has many drawbacks; for example, the soil infiltration system has a low environmental carrying capacity, covers a large area, and is easily blocked; the constructed wetland technology has problems, such as a low environmental pollution load and difficult operation in winter. Compared with land treatment technology, an aerated biological filter has the advantages of a small footprint, simple operation and maintenance, easy replacement of fillers, and high efficiency [9–12]. It has a good application prospect in rural decentralized domestic sewage treatment.

A biofilter is an artificial biological treatment technology developed based on the principle of soil self-purification through an intermittent sand and contact filter [13]. The filler is an important part of the biofilter. Studies have shown that the biofilter with traditional crushed stone or sand as the filler can effectively remove organic pollutants; however, the removal rate of nitrogen and phosphorus is low [14]. The biological filter itself belongs to the biofilm process, the treatment load is relatively low, and the upper limit of influent quality should not be too high. Nitrogen and phosphorus absorption by filter media includes the physical adsorption of a specific surface area and chemical adsorption in the form of ion interaction, and the filter media significantly affect the formation and shedding of biofilm. Moore et al. [15] studied the effect of filter media size on nitrogen and phosphorus removal in a biological filter, and found that small particle filter media (1.5–3.5 mm) is beneficial for nitrogen removal but unsuitable for a high hydraulic load, whereas large particle filter media (2.5–4.5 mm) improve filter operating conditions, but are un conducive to nitrogen removal and SS removal. As the gap between the traditional single filter media is too small, when the filter load is too high, the excessive biofilm growth will cause the blockage of the filter, causing a short flow phenomenon, greatly reducing the effluent quality. Therefore, most biological filters are presently mainly used in water bodies with a low nitrogen and phosphorus concentration load. For example, Liu et al. [16] used a biologically aerated filter to purify naturally polluted river water, while Huang et al. [17] used a biological filter to purify domestic municipal sewage. Generally, the nitrogen and phosphorus concentration in the influent concentration of the biological filter does not exceed 50.0-mg/L and 6.0-mg/L, respectively. However, the concentration range of nitrogen and phosphorus in rural blackwater is generally 150-mg/L and 15-mg/L, respectively. There are few studies on biological filters teaching how to purify the water bodies with high nitrogen and phosphorus concentrations in rural blackwater. Given the problem of the high pollution of nitrogen and phosphorus in rural blackwater after septic tank treatment, this paper (1) introduced the concept of the “shape factor,” conducted optimization of the isotherm adsorption model combined with the kinetic equation to screen the biofilter fillers with better performance; (2) used an optimized combination of fillers to construct a biofilter to study the treatment effect of high-concentration blackwater. This work may provide technical support and reference for purifying and treating rural blackwater.

2. Materials and Methods

2.1. Experimental Materials

Experimental materials: zeolite, volcanic rock, sepiolite, ceramsite, anthracite, specific gravity > 1, granular, particle size after sieving was 2–5-mm; vermiculite, peat, specific gravity < 1, granular, particle size after sieving was 1–3-mm. All materials utilized were washed with clean water and dried before use. The blackwater used in the test was obtained from the septic tanks of farmers in Ninghe District, Tianjin, China. The distribution of sampling points is shown in Figure 1, and the water quality indicators are shown in Table 1.



Figure 1. Distribution of collecting black water in villages.

Table 1. Influent (blackwater) quality of Biofilter.

Water Quality Index	TN (Total Nitrogen) (mg·L ⁻¹)	NO ₃ ⁻ -N (Nitrate Nitrogen) (mg·L ⁻¹)	NH ₄ ⁺ -N (Ammonia Nitrogen) (mg·L ⁻¹)	TP (Total Phosphorus) (mg·L ⁻¹)	COD (Chemical Oxygen Demand) (mg·L ⁻¹)	pH
Zhang laozhuang village (117°49" E, 39°44" N)	133 ± 5.4	1.3 ± 0.5	125 ± 6.4	7.8 ± 1.0	346 ± 9.4	7.5 ± 0.2
Da zhangzhuang village (117.45" E, 39°42" N)	151 ± 7.3	2.7 ± 0.4	137 ± 5.7	9.6 ± 0.8	354 ± 10.3	7.6 ± 0.3
Dong tazhaung village (117°47" E, 39°43" N)	127 ± 6.7	3.1 ± 1.2	115 ± 6.7	8.4 ± 1.1	369 ± 6.1	7.8 ± 0.3
Mao jiazhuang village (117°47" E, 39°42" N)	146 ± 10.3	1.5 ± 0.7	141 ± 9.6	12.5 ± 2.3	351 ± 7.2	7.2 ± 0.1
Dong guanzhuang village (117°48" E, 39°40" N)	151 ± 9.9	2.6 ± 1.1	135 ± 5.1	13.3 ± 1.6	367 ± 3.6	7.5 ± 0.4
Dong huaizhuang village (117°46" E, 39°41" N)	146 ± 5.7	2.1 ± 0.8	132 ± 7.2	6.7 ± 1.4	344 ± 5.6	7.6 ± 0.2
Dong mazhuang village (117°46" E, 39°40" N)	154 ± 8.3	3.5 ± 0.5	139 ± 5.8	13.8 ± 0.9	337 ± 4.2	7.9 ± 0.2
Lang erwo village (117°48" E, 39°40" N)	136 ± 6.5	1.6 ± 0.6	124 ± 4.4	10.7 ± 2.4	361 ± 5.1	7.9 ± 0.1
Dong baizhuang village (117°50" E, 39°41" N)	142 ± 7.2	1.8 ± 0.4	122 ± 10.1	6.5 ± 1.2	358 ± 4.3	7.6 ± 0.3
Influent concentration	145~156	1.5~3.4	126.4~137.1	8.9~12.1	341~362	7.2~7.9

2.2. Experimental Methods

2.2.1. Biofilter Filler Comparison Test

(1) Isothermal adsorption test of nitrogen and phosphorus by filler

NH_4Cl (ammonia chloride) (KH_2PO_4 (potassium dihydrogen phosphate)) solutions with concentrations of 10, 20, 40, 60, 80, 100, 150 and $200\text{-mg}\cdot\text{L}^{-1}$ were prepared in a 250 mL conical flask. Approximately 10-g filler was added, and the flask was placed in a thermostatic oscillator to shake for 24 h at $25\text{ }^\circ\text{C}$ and $125\text{ r}\cdot\text{min}^{-1}$. After removing the conical flask, 50-mL shaken liquid was transferred into a centrifuge tube and centrifuged for ten minutes at $4000\text{ r}\cdot\text{min}^{-1}$. The supernatant was filtered with a $0.45\text{-}\mu\text{m}$ microporous water-based filter membrane. The filtered liquid was subjected to nitrogen and phosphorus mass concentration determination, and the adsorption capacity of the filler was calculated. Three groups of parallel tests were established for each filler.

(2) Adsorption kinetics test for fillers for nitrogen and phosphorus

The NH_4Cl (KH_2PO_4) solution with a $50\text{ mg}\cdot\text{L}^{-1}$ concentration was prepared and placed in six 250-mL conical flasks. Each flask was added with 10-g filler and placed in a thermostatic oscillator for 24 h at $25\text{ }^\circ\text{C}$ and $125\text{ r}\cdot\text{min}^{-1}$. The six conical flasks were removed after 10, 20, 40, 60, 120 and 240 min. About 50-mL shaken liquid was placed into a centrifuge tube and centrifuged for ten minutes at $4000\text{ r}\cdot\text{min}^{-1}$. The supernatant was filtered with a $0.45\text{-}\mu\text{m}$ microporous water-based filter membrane. The filtered liquid was subjected to nitrogen and phosphorus mass concentration determination, and the adsorption capacity of the filler was calculated. Three groups of parallel tests were established for each filler.

2.2.2. Removal of Nitrogen and Phosphorus from Blackwater by the Biological Filter

The comparison of fillers revealed that vermiculite and zeolite are fillers with better nitrogen adsorption while peat and ceramsite, are fillers with better phosphorus adsorption. These fillers were combined in pairs, meaning that vermiculite + peat, zeolite + peat, zeolite + ceramsite, and vermiculite + ceramsite were used to construct aerated biofilters (the device is shown in Figure 2). The test device was a plexiglass column with a diameter of $\varnothing 0.4\text{ m} \times 0.5\text{ m}$, the water flow direction was an upward flow, and an aeration pump performed the aeration method at the bottom of the device for blast aeration. The air-water ratio of the device was 1:1, and the filler in the filter tank was filled with two different combinations of fillers evenly mixed at a volume of 1:1. The operating parameters of the aerated biofilter for purifying the actual blackwater were a hydraulic retention time of two hours, a hydraulic load P_{of} of $2\text{ m}^3/\text{m}^2/\text{h}$, and an aeration volume of 25 L/h . After the system was stable, the inflow and outflow water samples were obtained daily to determine the nitrogen and phosphorus contents.

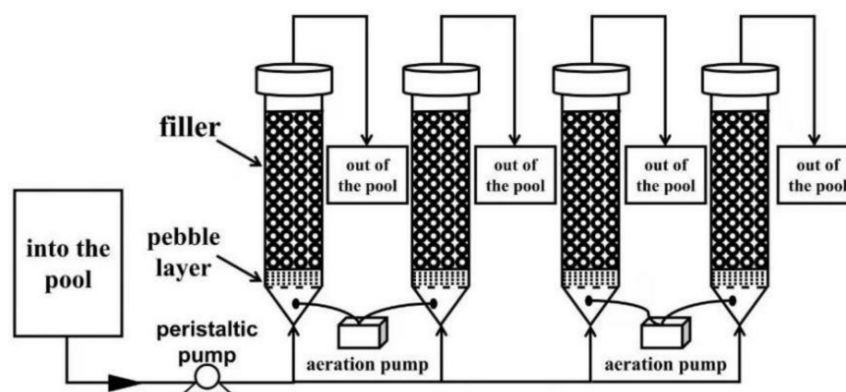


Figure 2. Biofilter test device.

2.2.3. Required Model Method for Fillers

(1) Optimization of the isotherm adsorption model

A. Basic model

For the adsorption phenomenon on the solid surface at a constant temperature, the Langmuir and Freundlich equations are often used to express the relationship between the adsorption amounts on the surface and the equilibrium concentration of the solute in the medium [18,19]. The distribution of adsorption sites during the nitrogen and phosphorus adsorption process by different materials was assessed following the fitted correlation coefficient.

The equilibrium adsorption capacity Q_e ($\text{mg}\cdot\text{kg}^{-1}$) of the filler for nitrogen and phosphorus was calculated using the following formula:

$$Q_e = \frac{V(C_0 - C_e)}{M} \quad (1)$$

where V is the volume of the solution, L ; C_0 is the nitrogen and phosphorus content in the initial solution, $\text{mg}\cdot\text{L}^{-1}$; C_e is the nitrogen and phosphorus content in the filtered liquid, $\text{mg}\cdot\text{L}^{-1}$; and M is the amount of filler, kg .

The Langmuir and Freundlich equations fitted the adsorption isotherm equations.

Langmuir equation:

$$Q_e = \frac{KQ_m C_e}{1 + KC_e} \quad (2)$$

Freundlich equation:

$$Q_e = kC_e^{\frac{1}{n}} \quad (3)$$

where Q_e is the adsorption amount of nitrogen and phosphorus by the filler, $\text{mg}\cdot\text{kg}^{-1}$; K is a constant that varies with the properties of the material; Q_m is the theoretical maximum nitrogen and phosphorus adsorption capacity by the filler, $\text{mg}\cdot\text{kg}^{-1}$; C_e is the equilibrium mass concentration of the solution, $\text{mg}\cdot\text{L}^{-1}$; k is the equilibrium adsorption coefficient reflecting the adsorption capacity of the filler; and n is the constant representing the adsorption strength of the filler.

B. Optimization model

The Langmuir and Freundlich equations are the gas–solid adsorption models derived by the physical chemist Langmuir based on the data results and the kinetics of adsorption when the physical chemist Langmuir studied the adsorption of low-pressure gases on metals. Researchers refer to this equation to explain the application of liquid–solid adsorption. This equation describes the adsorption state of the adsorbate on the pure substance and the equilibrium adsorption state without external interference. In this experiment, nitrogen and phosphorus adsorption by different materials was affected by the physical and chemical properties of many materials and the surrounding environmental factors, causing complex adsorption mechanisms and processes, which were difficult to quantify.

Thus, the concept of “shape factor” was introduced based on the Langmuir equation. “Shape factor” comes from population ecology. In population ecology, the logistic model is often used to describe the dynamic characteristics of the population. However, population growth is affected by several factors, so the model cannot fit the actual dynamics of the population properly [20]. Therefore, the concept of “shape factor” was introduced based on the logistic model [21]. Similarly, the adsorption model formed by introducing the “shape factor” into the Langmuir equation is as follows:

$$Q_e = \left(\frac{mKC_e}{1 + KC_e} \right)^d \quad (4)$$

where d is the shape factor introduced to reflect the influence of the physical and chemical properties of the adsorbent and environmental factors on the shape of the adsorption

isotherm; m is a parameter related to the saturated adsorption capacity; K is a constant that varies with material properties; and C_e is the equilibrium mass concentration of the solution, $\text{mg}\cdot\text{L}^{-1}$.

When the shape factor was 1, the constructed adsorption model was transformed into the Langmuir equation; when K was small, i.e., $1 + KC_e \approx 1$, the constructed adsorption model was transformed into the Freundlich equation. The optimized new equation model can determine the comprehensive influence degree of the material itself on the adsorption process according to the fitted d value. When the d value significantly deviates from 1, it indicates that the material significantly influences the adsorption process.

2.2.4. Adsorption Kinetic Analysis Method

The first-order kinetic equation, the double constant equation, and the Elovich equation are often used to describe the adsorption kinetics of the adsorbent on the adsorbate. The first-order kinetic equation is based on the regulation relationship between reactant concentration and reaction rate. The double constant equation reflects the complex kinetic fitting of the adsorption process. The Elovich equation reflects several reaction mechanisms in the adsorption process, and the activation energy changes significantly during the adsorption process. Using the kinetic equations mentioned above to simulate the kinetic process of nitrogen and phosphorus adsorption by the filler, the specific kinetic behavior of the filler in nitrogen and phosphorus adsorption can be assessed [22–24]. The specific equations are as follows:

First-order kinetic equation:

$$\ln Q_e = a + kt \quad (5)$$

Double constant equation:

$$\ln Q_e = a + k \ln t \quad (6)$$

Elovich equation:

$$Q_e = a + k \ln t \quad (7)$$

where Q_e is the equilibrium adsorption capacity of nitrogen and phosphorus by the filler, $\text{mg}\cdot\text{kg}^{-1}$; t is the adsorption time, min; a is a constant related to the initial concentration; and k is the rate constant related to the activation energy of adsorption.

2.2.5. Determination Method of Indicators

TN was determined using alkaline potassium persulfate spectrophotometry, ammonia nitrogen was determined using Na reagent spectrophotometry, nitrate-nitrogen was determined using ultraviolet spectrophotometry, and TP was determined using ammonium molybdate spectrophotometry. The fillers' surface area and pore size distribution were determined by a specific surface area and pore size analyzer. The fillers' surface characteristics were analyzed using scanning electron microscopy. The elemental composition of the material surface was determined using X-ray diffraction.

2.2.6. Data Analysis Method

The experimental data were sorted using Microsoft Excel 2019 (Microsoft, Redmond, WA, USA) and analyzed using Origin 2019. The Origin 2019 software was used for drawing.

3. Results and Discussion

3.1. Analysis of the Physical and Chemical Properties of Fillers

The seven materials' physical and chemical properties were analyzed and compared. The SEM (scanning electron microscope) analysis results of the fillers (Figure 3) show that the surfaces of zeolite, volcanic rock, ceramsite, peat, and vermiculite were relatively loose and rough, with numerous uneven folds and similar irregular scales on the surface, indicating that the materials had many active sites and could be used as the carriers for microbial attachment. The seven materials' chemical properties also differed. From the energy spectrum analysis of the seven materials (Figure 4), the surface of zeolite,

volcanic rock, ceramsite, and vermiculite had several types of elements, while the surface of sepiolite, anthracite, and peat had few types and contents of elements. Volcanic rock had the highest C content of 5.73%, followed by zeolite, ceramsite, and vermiculite (1.73–2.64%). The content of the O element in zeolite, volcanic rock, and ceramsite was 41.35–52.20%, followed by vermiculite (34.75%). The Si content of zeolite, ceramsite, and vermiculite was high, ranging from 18.56% to 35.05%. The content of Al in ceramsite reached 11.59%, followed by zeolite, volcanic rock, and vermiculite (7.77–9.02%). Additionally, the surface of volcanic rock, ceramsite, and vermiculite contained small amounts of elemental Fe, Mg, and Ca. The microstructures of the seven materials (Table 2) revealed that zeolite and vermiculite had the largest specific surface areas, which were 8.56 m²/g and 8.62 m²/g, respectively. The larger specific surface area could provide more adsorption sites for the filler, which benefited the physical adsorption of nitrogen and phosphorus elements in the water body. Ceramsite, zeolite, vermiculite, and the peat had a large pore volume and size.

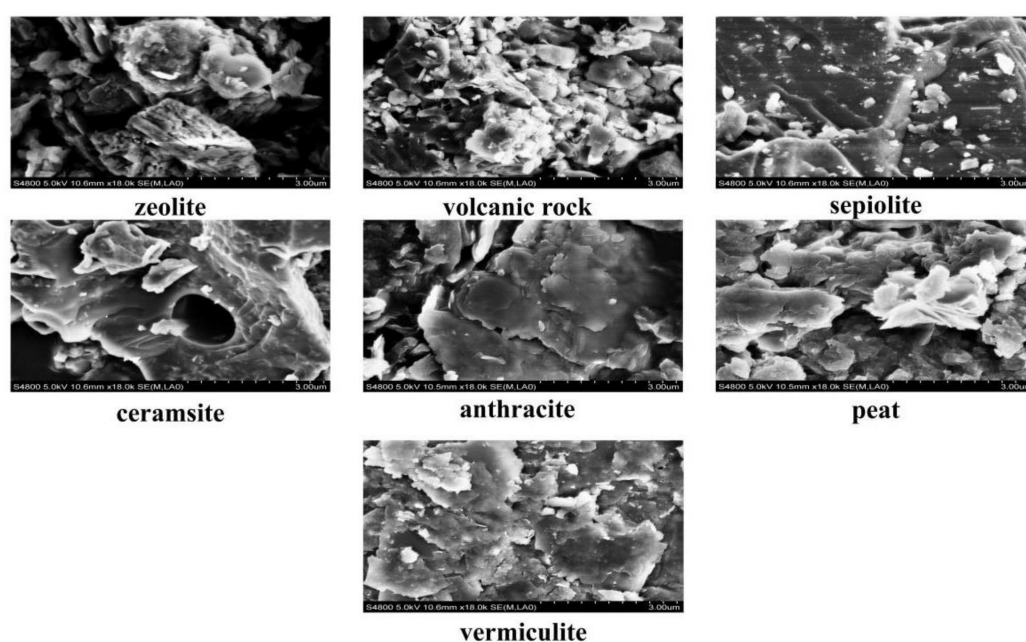


Figure 3. SEM (scanning electron microscope) images of the seven fillers.

Table 2. Physical and chemical properties of fillers Physic.

Parameter	Zeolite	Volcanic Rock	Sepiolite	Ceramsite	Anthracite	Peat	Vermiculite
specific surface area (m ² /g)	8.56	5.25	0.71	7.66	3.81	2.67	8.62
Micropore volume (cm ³ /g)	2.08×10^{-2}	1.67×10^{-2}	8.26×10^{-4}	7.15×10^{-2}	3.58×10^{-3}	2.85×10^{-2}	2.26×10^{-2}
micropore size (nm)	9.75	12.75	4.68	9.24	3.76	8.74	9.86
pH	7.68	10.58	8.87	9.54	7.82	6.67	7.35

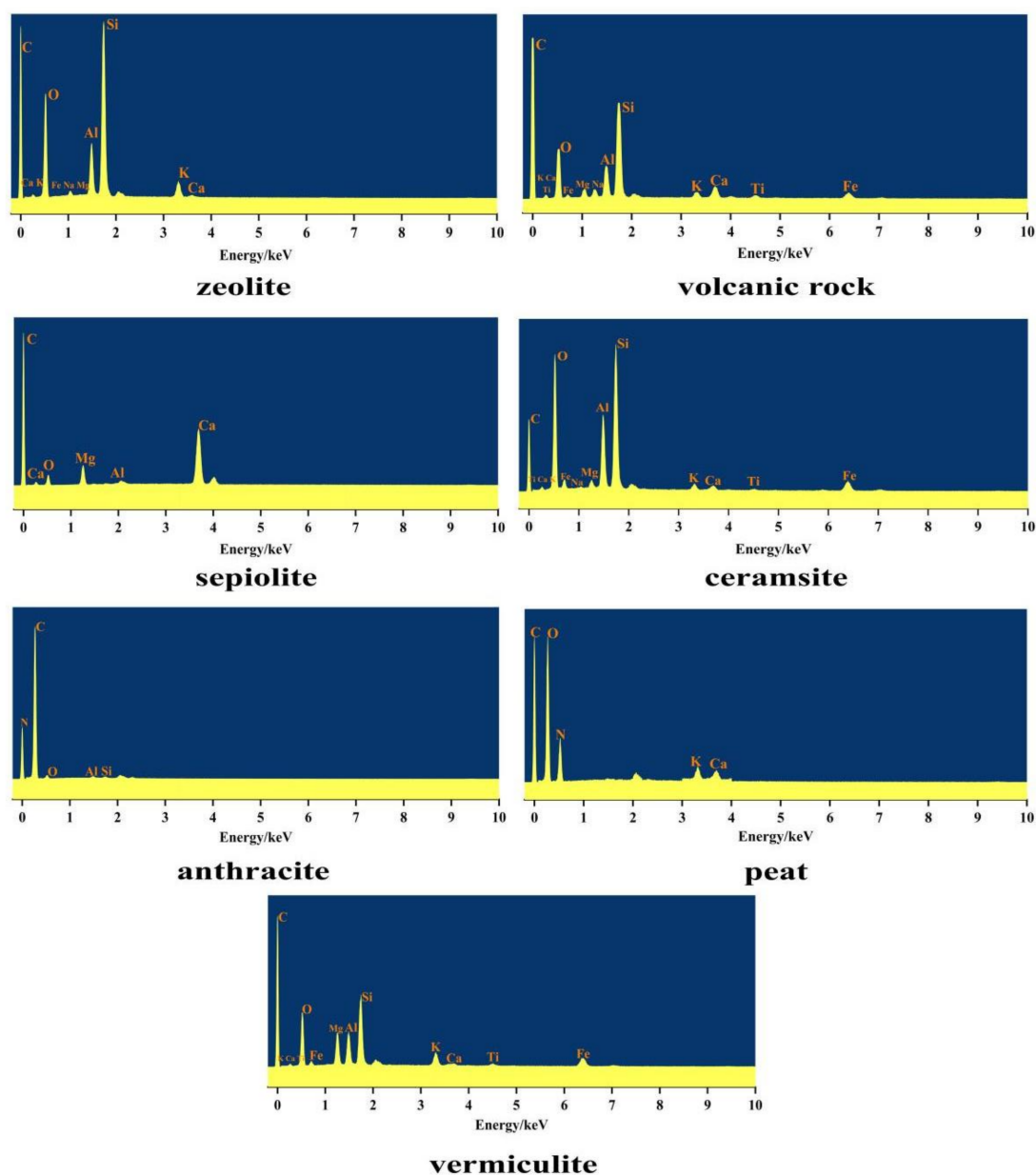


Figure 4. EDS (energy dispersive spectrum) spectrogram of the seven fillers.

3.2. Isothermal Adsorption Characteristics of the Seven Fillers for Nitrogen and Phosphorus

The isotherm adsorption curves were drawn based on the adsorption capacity and equilibrium concentration of nitrogen and phosphorus by each filler under different nitrogen and phosphorus solution concentrations (Figure 5). There were large differences in the adsorption capacity of nitrogen among the seven fillers. The adsorption trend increased with an increasing initial concentration, among which the adsorption capacities of vermiculite and peat were the largest. The nitrogen adsorption capacity of the seven materials was ranked as follows (from strong to weak): vermiculite > peat > zeolite > volcanic rock > sepiolite > anthracite > ceramsite. The adsorption isotherm curve of vermiculite had the largest slope, and the adsorption rate of nitrogen was also large. A $23.5\text{-mg}\cdot\text{L}^{-1}$ equilibrium concentration could still show a strong nitrogen adsorption capacity; the lower nitrogen adsorption capacity of peat compared to vermiculite may be due to the existence of other forms of nitrogen in peat, which interfered with the adsorption of nitrogen in the added liquid by peat [22]. Nitrogen removal using the filler is mainly through physical adsorption and ion exchange. The former occurs on the surface of the aluminosilicate

structure, and the latter occurs in the interior of the aluminosilicate structure. Nitrogen removal using ion exchange has strong stability [23]. In this study, vermiculite, peat, and zeolite presented high adsorption performance for nitrogen. The high adsorption performance of vermiculite and zeolite for nitrogen may be attributed to their rough surfaces and being porous, as well as their large specific surface area, which could benefit adsorption. Moreover, they could exchange ions with NH_4^+ (ammonia ion) in water without altering their crystal structure [24]. Both vermiculite and peat have a porous aluminosilicate crystal structure, containing many cavities and pores; its surface, with a strong dispersion force and cation exchange performance for NH_4^+ , demonstrates strong adsorption. However, in this experiment, the volcanic rock also had a rough surface and a large specific surface area, but a low adsorption performance for nitrogen, which may be because the volcanic rock will increase its pH when it is transferred into a water body, so OH^- (hydroxide ion) combined with NH_4^+ in the water body weakens the exchange capacity of cations inside the material and affects NH_4^+ adsorption [25].

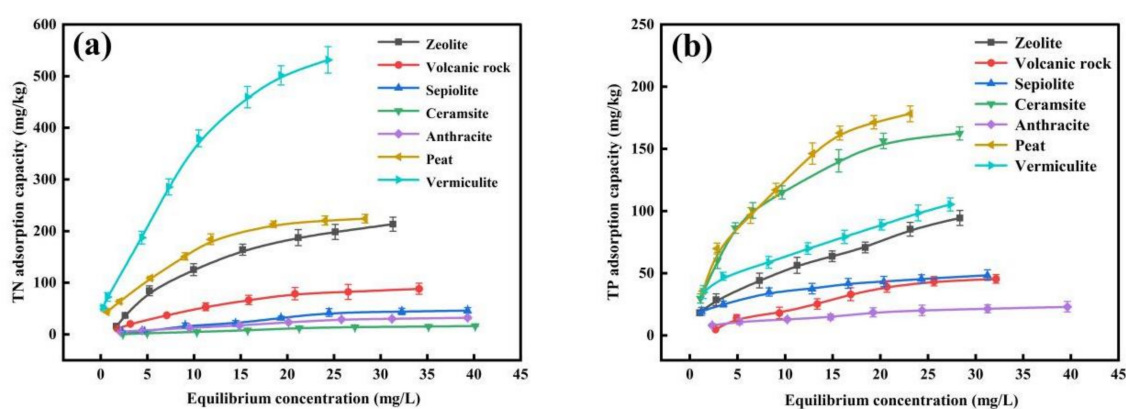


Figure 5. Isothermal adsorption curves of the seven fillers for nitrogen and phosphorus; (a) nitrogen, (b) phosphorus.

The adsorption capacity of the seven fillers to phosphorus increased with the increased initial concentration; the adsorption capacity of the peat to TP was the largest, because the specific surface area of the peat was large, and the adsorption performance was high (Figure 5). Additionally, the groups on the surface of peat displayed a certain chemical adsorption on P, and the ion exchange of Ca^{2+} (calcium ion) and K^+ (potassium ion) on phosphate in peat increased the adsorption capacity of phosphorus. The phosphorus adsorption capacity of the seven materials was ranked as follows (from strong to weak): peat > ceramsite > vermiculite > zeolite > sepiolite > volcanic rock > anthracite. The adsorption capacity and the adsorption rate of peat and ceramsite were basically similar when the equilibrium concentration of TP was $<9.5 \text{ mg}\cdot\text{L}^{-1}$; when the equilibrium concentration was higher than $9.5 \text{ mg}\cdot\text{L}^{-1}$, the adsorption rate of peat was gradually higher than that of ceramsite with an increased phosphorus equilibrium concentration. The phosphorus removal using fillers was through surface adsorption and precipitation [26,27]. The Ca^{2+} , Fe^{2+} (iron ion), Mg^{2+} (magnesium ion), and Na^+ (sodium ion) plasmas contained in the filler were released into the water body and formed a poorly soluble compound with phosphorus in the water body; phosphorus was exchanged with the abovementioned metal ions hydrated on the surface of the material and bound into the crystal lattice of the material [28,29]. Ceramsite contains a large amount of Ca^{2+} , Fe^{2+} , Mg^{2+} , and Na^+ so the removal effect of the collar in the water body was better [30]. The removal effect of peat on phosphorus was better than that of other materials, partly because peat has a rough surface and a large specific surface area, causing greater physical adsorption. A high physical adsorption was more conducive to phosphorus adsorption in water on its surface and promoted the physicochemical role of relevant metal ions and phosphorus. Some studies have also shown that crystalline soil minerals, iron and aluminum oxides,

organic matter, and other substances in peat have a high affinity for PO_4^{3-} (phosphate ion). Particularly, amorphous iron and aluminum oxides have a strong adsorption effect on phosphorus [31,32].

The isotherm adsorption curves of nitrogen and phosphorus by each filler were fitted with the basic and optimized model. The results are shown in Table 3. In the basic model, the K value represents the adsorption and binding capacity of the material, and the adsorption and binding capacity of the filler for nitrogen was as follows: peat > vermiculite > volcanic rock > zeolite > anthracite > sepiolite > ceramsite; Q_m represents the theoretical adsorption saturation of nitrogen, and the theoretical adsorption saturation of nitrogen from large to small was as follows: vermiculite > zeolite > peat > sepiolite > volcanic rock > ceramsite > anthracite. K is a constant that reflects the nitrogen adsorption capacity of the filler. Theoretically, the larger the k value, the better the nitrogen adsorption capacity of the filler. Among the seven fillers, vermiculite and peat had higher k values, followed by zeolite and volcanic rock. To summarize, vermiculite and peat exhibited better nitrogen adsorption among the seven fillers. In the isotherm fitting of phosphorus adsorption, the Freundlich ($R^2 > 0.90$) equation could better fit the phosphorus adsorption characteristics of the seven fillers, while the Langmuir ($R^2 > 0.90$) equation only fitted the adsorption characteristics of phosphorus on five fillers, except for vermiculite and anthracite. These findings indicated that the adsorption characteristics of vermiculite and anthracite were more inclined to multilayered molecular adsorption. In the phosphorus Langmuir equation, the K values of the seven fillers from large to small were as follows: sepiolite > vermiculite > anthracite > zeolite > ceramsite > peat > volcanic rock; the order of Q_m was peat > ceramsite > volcanic rock > vermiculite > zeolite > sepiolite > anthracite. In the Freundlich equation, the k value of ceramsite, peat, and vermiculite was large; that is, the adsorption capacity of phosphorus was large. Hence, among the seven fillers, ceramsite and peat exhibited a better adsorption performance for phosphorus.

Table 3. The isotherm adsorption equation of 7 kinds of fillers for nitrogen and phosphorus.

Filler	Langmuir Adsorption Model			Freundlich Isotherm Adsorption			
	Q_m ($\text{mg}\cdot\text{kg}^{-1}$)	K	R^2	k	n	R^2	
TN	Zeolite	300.885	0.028	0.981	10.568	1.269	0.982
	Volcanic rock	179.279	0.037	0.978	8.770	1.371	0.981
	Sepiolite	276.860	0.007	0.951	1.920	1.080	0.930
	Ceramsite	145.711	0.004	0.954	0.505	1.022	0.932
	Anthracite	94.308	0.017	0.975	2.251	1.284	0.968
	Peat	290.062	0.131	0.960	48.993	1.981	0.974
	Vermiculite	654.496	0.129	0.973	147.694	1.320	0.979
TP	Zeolite	90.404	0.159	0.960	17.511	2.095	0.967
	Volcanic rock	218.068	0.010	0.963	2.644	1.129	0.965
	Sepiolite	46.155	0.428	0.928	17.931	3.382	0.916
	Ceramsite	233.884	0.129	0.972	34.517	1.853	0.973
	Anthracite	23.303	0.163	0.853	5.338	2.463	0.952
	Peat	282.409	0.088	0.939	31.475	1.644	0.950
	Vermiculite	94.873	0.289	0.878	29.105	2.781	0.940

Based on the adsorption test results of nitrogen and phosphorus on seven different materials, nonlinear parameter estimation was conducted on Origin software using the optimized isotherm adsorption model (Table 4). In the new adsorption equation model, each material's correlation coefficient of nitrogen and adsorption could reach a significant level. The average value of the correlation coefficient in Table 3 was 0.984, which showed that the new adsorption equation model demonstrated a good fitting degree. The new isothermal adsorption equation could assess the comprehensive influence of the material itself on the adsorption process following the fitted d value. The greater the deviation of d from 1, the greater the comprehensive influence of the nature of the filler itself on the

adsorption process to further screen the materials with better adsorption performance. In this experiment, given that the environmental conditions of different materials in the adsorption process were similar, the fitted d value of the properties of zeolite (1.037) and vermiculite (0.995) minimally affected nitrogen adsorption, while ceramsite (1.034) and peat (0.944) slightly affected phosphorus adsorption.

Table 4. The isothermal adsorption equation of nitrogen and phosphorus by 7 kinds of fillers under the new equation model.

Filler	TN				TP			
	m	K	d	R^2	m	K	d	R^2
Zeolite	289.76	0.036	1.037	0.999	157.21	0.012	0.978	0.998
Volcanic rock	32.70	0.022	1.534	0.987	1034.14	0.009	0.832	0.975
Sepiolite	74.92	0.034	1.275	0.994	967.31	0.017	0.773	0.943
Ceramsite	4217.62	0.006	0.703	0.973	193.44	0.008	1.034	0.998
Anthracite	967.34	0.004	0.671	0.981	12.71	0.021	1.231	0.977
Peat	133.92	0.031	1.125	0.998	319.61	0.008	0.944	0.998
Vermiculite	1367.95	0.002	0.995	0.998	612.34	0.032	0.729	0.981

Vermiculite and zeolite, with a better nitrogen adsorption effect, and the ceramsite and peat, with a better phosphorus adsorption effect, were subjected to SEM analysis after their adsorption, and the results are shown in Figure 6. After vermiculite adsorbed nitrogen, a large amount of particulate matter aggregated on its surface and appeared as a spiderweb-like polymer. Compared with the unadsorbed zeolite, its surface voids were basically filled, and many white particulate matter clusters were attached to its surface. Similarly, the voids on the surface were largely covered for ceramsite and peat with a remarkable phosphorus adsorption effect, and more particulate matter was attached after phosphorus adsorption. Conversely, the metal ions and functional groups in the gap or surface of the filler had an exchange adsorption reaction with the nitrogen and phosphorus in the water. Alternatively, many particles attached to the surface of the filler played a strong ion physical adsorption role using the adsorption site of the filler itself.

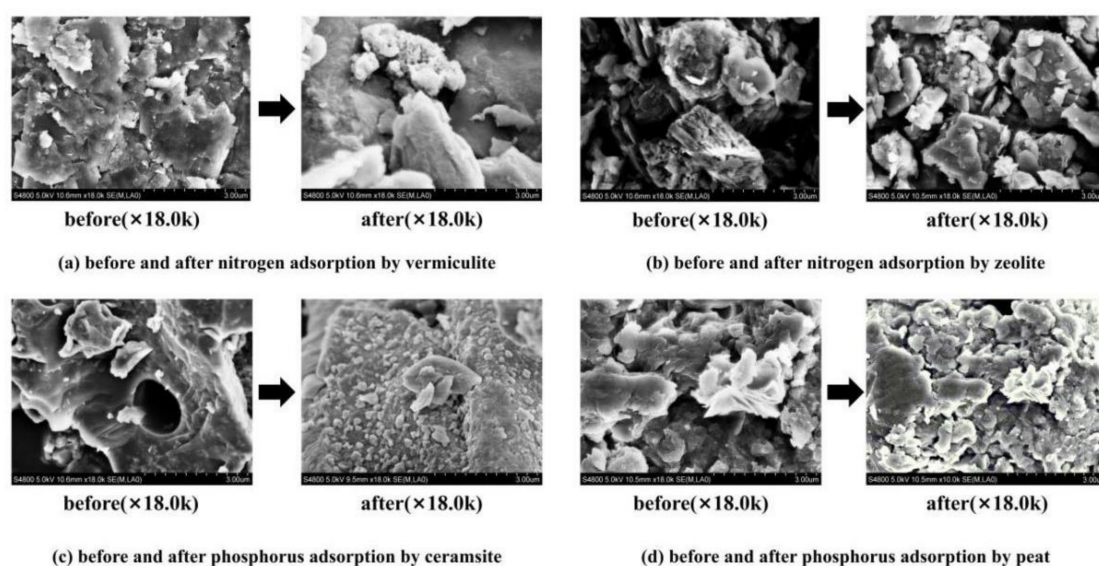


Figure 6. Surface characteristics of different fillers after adsorption of nitrogen and phosphorus; (a) before and after nitrogen adsorption by vermiculite, (b) before and after nitrogen adsorption by zeolite, (c) before and after phosphorus adsorption by ceramsite, (d) before and after phosphorus adsorption by peat.

3.3. Adsorption Kinetics of Nitrogen and Phosphorus with Seven Fillers

Under different nitrogen and phosphorus concentrations, the dynamic change process of nitrogen and phosphorus adsorption by different materials with time is shown in Figure 7. The adsorption amount of nitrogen by the seven fillers changed with time, showing a trend of first increasing and then decreasing until a slow equilibrium was reached. From 10–60 min, the adsorption rate of nitrogen to each filler was fast. At this time, many idle adsorption sites were found on the surface of the filler, and nitrogen in the solution could quickly occupy the idle sites to show a rapid adsorption rate. In 60–120 min, except for the increase in the sepiolite adsorption rate, the nitrogen adsorption rates of the other fillers decreased to varying degrees. With the progress of the adsorption process, the free adsorption sites were gradually occupied, and the filler could only increase the adsorption amount by replacing the ammonium ions in the solution with exchangeable cations in its spatial structure, causing a gradual slowdown of the adsorption rate. In 120–240 min, the adsorption rate of nitrogen on the seven fillers gradually decreased to 0, when the space sites on the surface of the fillers were all occupied, and the exchangeable cations in the space structure were all replaced to achieve the adsorption dynamic equilibrium. The change in the nitrogen adsorption rate with time for the seven fillers was consistent with the results obtained by Zhu et al. (2011) [33]. The kinetic adsorption process of phosphorus on the seven fillers exhibited the same three stages of fast, medium, and slow, indicating high, medium, and low energy adsorption sites on the surface of the fillers. Among the seven fillers, ceramsite had the fastest adsorption rate of phosphorus, followed by peat and zeolite.

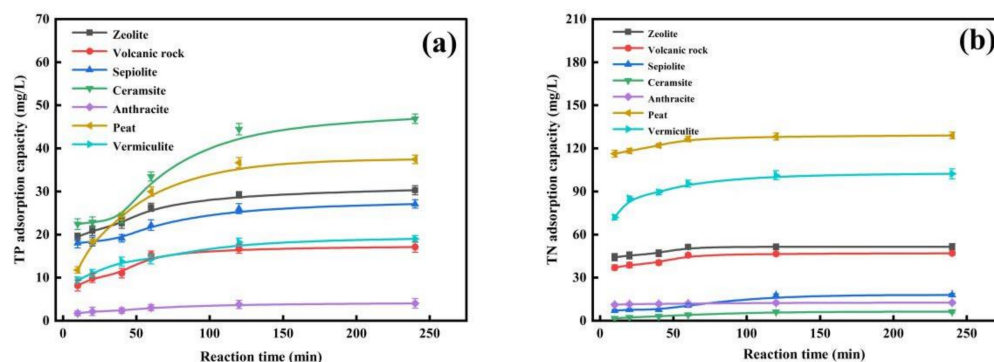


Figure 7. Adsorption kinetics curves of nitrogen and phosphorus by the seven fillers; (a) nitrogen, (b) phosphorus.

The dynamic adsorption test data of seven fillers for nitrogen and phosphorus were analyzed using the first-order kinetic equation, double constant equation, and Elovich equation. Table 5 shows that the double constant equation and the Elovich equation could fit the nitrogen adsorption process of the seven fillers in the experiment sufficiently, and the fitting correlation coefficients all reached more than 0.80. The first-order kinetic equation only fits the adsorption process of ceramsite to nitrogen well, and the fitting coefficient could reach 0.959, indicating that the six materials except for ceramsite did not conform to the kinetic process of a single matrix reaction, but were more in line with the adsorption process, which is determined by multiple factors. The constant k in the double constant and Elovich equation represents the adsorption rate. The fitting results demonstrated that the adsorption rates of the seven fillers to nitrogen were as follows: vermiculite > peat > zeolite > volcanic rock > sepiolite > ceramsite > anthracite. The double constant and Elovich equation could better fit the adsorption process of phosphorus on the seven fillers, and the fitting coefficients could all be above 0.820. The first-order kinetic equation could only fit the adsorption process of peat on phosphorus well, and the fitting coefficient was 0.937, which was larger than the two other equations. Thus, the adsorption process of peat on phosphorus was more consistent with the kinetic process of the single-substrate reaction,

and the adsorption process of phosphorus on the six other fillers was a reaction mechanism with a more complex reaction and a large change in activation energy during the reaction. The k value in the fitting equation indicated that the adsorption rates of phosphorus on the seven fillers from large to small were as follows: peat > ceramsite > zeolite > sepiolite > vermiculite > volcanic rock > anthracite.

Table 5. Fitting results of the adsorption kinetics of seven kinds of fillers on TN and TP.

Filler	First-Order Model			Double Constants			Models of Elovich			
	a	k	R^2	a	k	R^2	a	k	R^2	
TN	Zeolite	49.681	0.205	0.3608	3.668	0.054	0.807	36.198	3.963	0.847
	Volcanic rock	44.362	0.159	0.407	3.426	0.083	0.857	228.727	3.556	0.869
	Sepiolite	18.021	0.022	0.758	1.001	0.354	0.879	−3.836	3.267	0.832
	Ceramsite	6.503	0.019	0.959	−0.271	0.402	0.909	−2.463	1.649	0.938
	Anthracite	12.066	0.249	0.361	2.32	0.04	0.987	10.054	0.47	0.987
	Peat	125.144	0.254	0.35	4.674	0.036	0.908	106.008	4.464	0.915
	Vermiculite	96.955	0.125	0.773	4.111	0.101	0.877	54.102	9.468	0.909
TP	Zeolite	27.218	0.095	0.466	2.607	0.152	0.939	10.102	3.772	0.942
	Volcanic rock	16.397	0.044	0.787	1.633	0.233	0.859	0.776	3.148	0.897
	Sepiolite	23.524	0.11	0.218	2.475	0.153	0.899	9.133	3.254	0.873
	Ceramsite	44.607	0.029	0.593	2.314	0.286	0.872	−2.45	8.927	0.828
	Anthracite	3.764	0.035	0.761	−0.054	0.272	0.943	−0.185	0.777	0.947
	Peat	37.007	0.03	0.973	2.038	0.305	0.881	−7.314	8.662	0.957
	Vermiculite	17.31	0.052	0.707	1.768	0.222	0.953	1.77	3.216	0.966

3.4. Removal Effect of Four Combined Fillers of Biofilter on Nitrogen and Phosphorus in Black Water

The fitting results of the adsorption saturation value of the filler and the adsorption rate showed that the fillers with better removal effects of nitrogen and phosphorus were vermiculite, zeolite, peat, and ceramsite. The four fillers were compounded and combined (vermiculite + peat, zeolite + peat, zeolite + ceramsite, and vermiculite + ceramsite) to construct a biofilter. The removal effect of nitrogen and phosphorus in blackwater is shown in Figure 8. In the first five days of each group of packed biofilters, the nitrogen removal rate showed a gradually increasing trend; from five days to 16 days, the nitrogen removal rate decreased and fluctuated to a certain extent; after 16 days, the nitrogen removal rate began to increase and basically stabilize. After a stable operation, the influent TN concentration of each combination of fillers was 152–160 mg·L^{−1}. The average effluent TN concentrations were 120.28, 58.88, 44.89 and 90.77 mg·L^{−1}, and the average removal rates of TN were 22.72%, 63.16%, 71.28% and 41.79%, respectively. The combination of zeolite + ceramsite had the best removal effect of nitrogen. In Section 3.1, vermiculite demonstrated the best adsorption performance for nitrogen. However, in actual sewage treatment, the combination of fillers mixed with vermiculite is not as good as the combination of fillers mixed with zeolite for nitrogen treatment. Vermiculite has a strong cation exchange performance, and the ion exchange process is mainly used in the adsorption test process, which can better adsorb NH₄⁺ [34]. However, nitrogen in the actual blackwater exists in various forms, such as organic nitrogen, nitrate nitrogen, nitrite nitrogen, and ammonia nitrogen, which can have an unsatisfactory effect of vermiculite on nitrogen removal in actual sewage treatment. Moreover, zeolite has a higher porosity and larger specific surface area than vermiculite [35,36]; in actual sewage treatment, the combination of fillers mixed with zeolite has a better TN removal effect. The filler combination of zeolite + ceramsite also showed the best removal effect of ammonia nitrogen in blackwater. The influent ammonia nitrogen concentration was 126–133 mg·L^{−1}, and the average removal rate of ammonia nitrogen was 78.92%, which was 58.89%, 12.05%, and 53.06% higher than other combinations, respectively. In blackwater with a high phosphorus concentration influent TP of 12 mg·L^{−1}, the average TP concentration in the effluent after the combined treatment of zeolite + ceramsite was 1.80 mg·L^{−1}. When the system ran stably, the TP removal effect

was stabilized at 73–75%, which was significantly higher than the biofilter with the three other combined fillers.

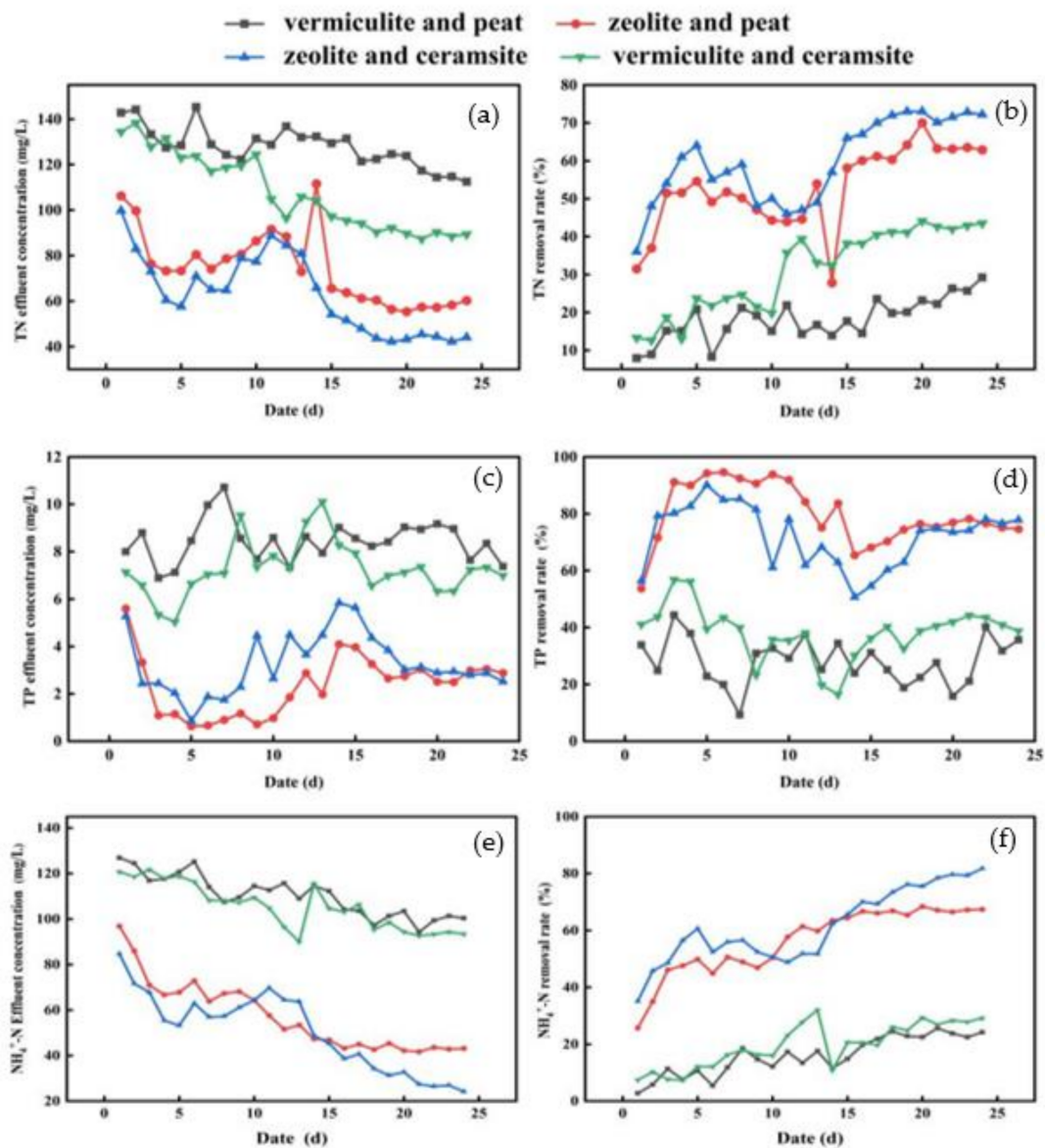


Figure 8. Adsorption kinetics curves of nitrogen and phosphorus by the seven fillers; (a) TN effluent concentration, (b) TN removal rate, (c) TP effluent concentration, (d) TP removal rate, (e) $\text{NH}_4^+\text{-N}$ effluent concentration, (f) $\text{NH}_4^+\text{-N}$ removal rate.

Presently, most biofilter technologies are used to treat rural domestic sewage with a low pollution load, as shown in Table 6. The concentration ranges of nitrogen and phosphorus in the influent were 9–50 mg/L and 1.3–4.0 mg/L, respectively, and the removal rates of nitrogen and phosphorus were 68–90% and 78–95%, respectively. This study used a biological filter to treat blackwater with a high pollution load in rural areas. Under the influent conditions of TN and phosphorus concentrations of 150–162 mg/L as well as 10–14 mg/L, the removal rates of nitrogen and phosphorus reached 71% and 73%, respectively. Thus, it can be seen that the biological filter packing combination selected in this study can carry a higher nitrogen and phosphorus load. The treated water could be directly used in forestry and animal husbandry in rural areas. Additionally, the effluent water quality could meet the secondary discharge standard of “Pollutant Discharge Standard for Urban Sewage Treatment Plant” (GB18918-2002) and the nitrogen as well as

phosphorus requirements in the “Surface Water Environmental Quality Standard” (GB 3838-2002) Class IV. Water resources can also be recycled. Subsequent experiments will continue to track and monitor the changes in the treatment effect of the biofilter under long periods. Additionally, the process operating parameters of the biofilter, such as the hydraulic retention time, gas–water ratio, and C/N ratio, can be optimized to further study the purification effect of a biological filter on blackwater.

Table 6. Fitting results of the adsorption kinetics of 7 kinds of fillers on TN and TP.

Filler	Types of Sewage	Influent TN/TP Concentration (mg/L)	Removal Rate (%)	Reference
quartz sand	secondary effluent of municipal sewage treatment plant	15.0 (TN)	89.4	[37]
gravel and immobilized biochar beads	simulated wastewater	13.0 (TN)	86.2	[38]
sulfur autotrophic denitrification composite	simulated wastewater	9.0–12.0 (TN)	81.1	[39]
ceramsite	urban sewage	40.0 (TN)	75.0	[40]
clay	simulated wastewater	35.0 (TN)	68.3	[41]
organic suspended	landfill leachate	35.0 (TN)	81.5	[42]
ceramisite and sulfur	synthetic municipal wastewater	50.0 (TN)	90.2	[43]
ZVI (zero-valent iron)/PHBV (3-hydroxybutyric acid-co-3-hydroxyvaleric acid copolyester)/sawdust composite	simulated wastewater	1.6 (TP)	98.5	[44]
quartz sand	simulated wastewater	4.0 (TP)	78.1	[45]
soil, plant detritus and eutrophic lake sediment	stormwater	1.3 (TP)	88.6	[46]

4. Conclusions

The adsorption rates of the seven fillers for nitrogen from high to low were vermiculite > peat > zeolite > volcanic rock > sepiolite > ceramsite > anthracite. The order of the adsorption rate of phosphorus was peat > ceramsite > zeolite > sepiolite > vermiculite > volcanic rock > anthracite. Additionally, vermiculite and zeolite slightly affected the adsorption process of nitrogen, and the theoretical saturated adsorption capacity was high at 654.50 and 300.89 mg·L⁻¹, respectively. Peat and ceramsite had little effect on the phosphorus adsorption process and high theoretical saturated adsorption, namely, 282.41 and 233.89-mg·L⁻¹, respectively. In the biofilter with four combined fillers, the filler combination of zeolite + ceramsite had a better removal effect of nitrogen and phosphorus in high-concentration blackwater; the removal rate of the system could attain 73–76%, and the nitrogen and phosphorus indicators in the effluent of the system could meet the requirements of general industrial water, recreational water, landscape water, forestry, and animal husbandry water standards in rural areas.

Author Contributions: Methodology, Writing, Supervision, Writing—Reviewing and Editing, P.C. Sampling, Data Management, Writing, and Software, D.C. Investigation, Formal Analysis, Visualization, W.Z. Conceptualization, Supervision and Validation, X.Z. All authors have read and agreed to the published version of the manuscript.

Funding: This study was funded and supported by the the Tianjin Natural Science Fund (19JCY-BJC23100), the Science and Technology Innovation Project from the Chinese Academy of Agricultural Sciences (CAAS-XTX2016015), and the Chinese Academy of Agricultural Sciences innovation engineering.

Informed Consent Statement: Informed consent was obtained from all subjects involved in the study.

Data Availability Statement: Data are contained within the article. For detailed information of each part, please contact the corresponding author.

Conflicts of Interest: These authors declare no conflict of interest.

References

1. Oarga, A.; Jenssen, P.D.; Bulc, T.G. A comparison of various bulking materials as a supporting matrix in composting blackwater solids from vacuum toilets. *J. Environ. Manag.* **2019**, *243*, 78–87. [[CrossRef](#)] [[PubMed](#)]
2. Cheng, F.K.; Dai, Z.Q.; Shen, S.; Wang, S.Y.; Lu, X.W. Characteristics of rural domestic wastewater with source separation. *Water Sci. Technol.* **2021**, *83*, 233–246. [[CrossRef](#)] [[PubMed](#)]
3. Hawkins, B.T.; Sellgren, K.L.; Cellini, E.; Klem, J.D.E.; Rogers, T.; Lynch, B.J.; Piascik, J.R.; Stoner, B.R. Remediation of suspended solids and turbidity by improved settling tank design in a small-scale, free-standing toilet system using recycled blackwater: Remediation of suspended solids and turbidity. *Water Environ. J.* **2019**, *33*, 61–66. [[CrossRef](#)] [[PubMed](#)]
4. Singh, R.P.; Kun, W.; Fu, D.F. Designing process and operational effect of modified septic tank for the pre-treatment of rural domestic sewage. *J. Environ. Manag.* **2019**, *251*, 109552. [[CrossRef](#)]
5. Mao, Y.X.; Tan, H.F.; Wang, K.M.; Zhang, Y.J.; Jin, Z.; Zhao, M.; Li, Y.Q.; Zheng, X.Y. Enhancement of algae ponds for rural domestic sewage treatment by prolonging daylight using artificial lamps. *Ecotoxicol. Environ. Saf.* **2021**, *228*, 113031. [[CrossRef](#)] [[PubMed](#)]
6. Dan, X.; Gao, L.R.; Zheng, M.H.; Li, J.G.; Zhang, L.; Wu, Y.N.; Qiao, L.; Tian, Q.C.; Huang, H.T.; Liu, W.B.; et al. Health risks posed to infants in rural China by exposure to short- and medium-chain chlorinated paraffins in breast milk. *Environ. Int.* **2017**, *103*, 1–7.
7. Yang, S.L.; Zheng, Y.F.; Mao, Y.X.; Xu, L.; Jin, Z.; Zhao, M.; Kong, H.N.; Huang, X.F.; Zheng, X.Y. Domestic wastewater treatment for single household via novel subsurface wastewater infiltration systems (SWISs) with NiiMi process: Performance and microbial community. *J. Clean Prod.* **2021**, *279*, 123434. [[CrossRef](#)]
8. Bradley, B.R.; Daigger, G.T.; Rubin, R.; Tchobanoglous, G. Evaluation of onsite wastewater treatment technologies using sustainable development criteria. *Clean Techn. Environ. Policy* **2002**, *4*, 87–99. [[CrossRef](#)]
9. Dong, J.X.; Wang, Y.H.; Wang, L.J.; Wang, S.J.; Li, S.J.; Ding, Y. The performance of porous ceramsites in a biological aerated filter for organic wastewater treatment and simulation analysis. *J. Water Process Eng.* **2020**, *34*, 101134. [[CrossRef](#)]
10. Wang, H.J.; Dong, W.Y.; Li, T.; Liu, T.Z. A modified BAF system configuring synergistic denitrification and chemical phosphorus precipitation: Examination on pollutants removal and clogging development. *Bioresour. Technol.* **2015**, *189*, 44–52. [[CrossRef](#)]
11. Zhang, L.L.; Yue, Q.Y.; Yang, K.L.; Zhao, P.; Gao, B.Y. Enhanced phosphorus and ciprofloxacin removal in a modified BAF system by configuring Fe-C micro electrolysis: Investigation on pollutants removal and degradation mechanisms. *J. Hazard Mater.* **2018**, *342*, 705–714. [[CrossRef](#)] [[PubMed](#)]
12. Ren, W.A.; Cao, F.F.; Ju, K.; Tang, F.B.; Chai, B.B.; Li, S.M.; Jin, P.K. Regulatory strategies and microbial response characteristics of single-level biological aerated filter-enhanced nitrogen removal. *J. Water Process Eng.* **2021**, *42*, 102190. [[CrossRef](#)]
13. Manirakiza, B.; Sirotkin, A.C. Bioaugmentation of nitrifying bacteria in up-flow biological aerated filter’s microbial community for wastewater treatment and analysis of its microbial community. *Sci. Afr.* **2021**, *14*, e00981. [[CrossRef](#)]
14. Lu, Z.D.; Sun, W.J.; Li, C.; Cao, W.F.; Jing, Z.B.; Li, S.M.; Ao, X.W.; Chen, C.; Liu, S.M. Effect of granular activated carbon pore-size distribution on biological activated carbon filter performance. *Water Res.* **2020**, *177*, 115768. [[CrossRef](#)] [[PubMed](#)]
15. Moore, R.; Quarmby, J.; Stephenson, T. The effects of media size on the performance of biological aerated filters. *Water Res.* **2001**, *35*, 2514–2522. [[CrossRef](#)]
16. Liu, H.Y.; Zhu, L.Y.; Tian, X.H.; Yin, Y.S. Seasonal variation of bacterial community in biological aerated filter for ammonia removal in drinking water treatment. *Water Res.* **2017**, *123*, 668–677. [[CrossRef](#)]
17. Huang, W.Y.; She, Z.L.; Gao, M.C.; Wang, Q.; Jin, C.J.; Zhao, Y.G.; Guo, L. Effect of anaerobic/aerobic duration on nitrogen removal and microbial community in a simultaneous partial nitrification and denitrification system under low salinity. *Sci. Total Environ.* **2019**, *651 Pt 1*, 859–870. [[CrossRef](#)]
18. Guo, X.; Wang, J.L. Comparison of linearization methods for modeling the Langmuir adsorption isotherm. *J. Mol. Liq.* **2019**, *296*, 111850. [[CrossRef](#)]
19. Kanô, F.; Abe, I.; Kamaya, H.; Ueda, I. Fractal model for adsorption on activated carbon surfaces: Langmuir and Freundlich adsorption. *Surf. Sci.* **2000**, *467*, 131–138. [[CrossRef](#)]
20. Ma, J.M.; Yuan, C.; Zhou, J.Y.; Li, Y.; Gao, G.Y.; Fu, B.J. Logistic model outperforms allometric regression to estimate biomass of xerophytic shrubs. *Ecol. Indic.* **2021**, *132*, 108278. [[CrossRef](#)]
21. Wang, Z.H.; Demarcy, T.; Vandersteen, C.; Gnansia, D.; Raffaelli, C.; Guevara, N.; Hervé, D. Bayesian logistic shape model inference: Application to cochlear image segmentation. *Med. Image Anal.* **2022**, *75*, 102268. [[CrossRef](#)] [[PubMed](#)]
22. Vassiljev, A.; Kaur, K.; Annus, I. Modelling of nitrogen leaching from watersheds with large drained peat areas. *Adv. Eng. Softw.* **2018**, *125*, 94–100. [[CrossRef](#)]
23. Jiang, C.; Jia, L.Y.; Zhang, B.; He, Y.L.; George, K. Comparison of quartz sand, anthracite, shale and biological ceramsite for adsorptive removal of phosphorus from aqueous solution. *J. Environ. Sci.* **2014**, *26*, 466–477. [[CrossRef](#)]
24. Wan, C.L.; Ding, S.; Zhang, C.; Tan, X.J.; Zou, W.G.; Liu, X.; Yang, X. Simultaneous recovery of nitrogen and phosphorus from sludge fermentation liquid by zeolite adsorption: Mechanism and application. *Sep. Purif. Technol.* **2017**, *180*, 1–12. [[CrossRef](#)]

25. Haruna, S.; Yoshinori, T.; Nanako, O.O.; Yoshito, C.; Naohiko, O. Nitrogen Isotopic Fractionation in Ammonia during Adsorption on Silicate Surfaces. *ACS Earth Space Chem.* **2017**, *1*, 24–29.
26. Drizo, A.; Frost, C.A.; Smith, K.A.; Grace, J. Phosphate and ammonium removal by constructed wetlands with horizontal subsurface flow, using shale as a substrate. *Water Sci. Technol.* **1997**, *35*, 95–102. [[CrossRef](#)]
27. Dong, C.S.; Ju, S.C.; Hong, J.L.; Jong, S.H. Phosphorus retention capacity of filter media for estimating the longevity of constructed wetland. *Water Res.* **2005**, *39*, 2445–2457.
28. Wang, Y.; Shen, Z.Y.; Niu, J.F.; Liu, R.M. Adsorption of phosphorus on sediments from the Three-Gorges Reservoir (China) and the relation with sediment compositions. *J. Hazard Mater.* **2009**, *162*, 92–98. [[CrossRef](#)]
29. Zhao, J.H.; Zhao, Y.Q.; Xu, Z.H.; Liam, D.; Liu, R.B. Highway runoff treatment by hybrid adsorptive media-baffled subsurface flow constructed wetland. *Ecol. Eng.* **2016**, *91*, 231–239. [[CrossRef](#)]
30. Shao, Q.; Zhang, Y.; Liu, Z.; Long, L.Z.; Chen, Y.Q.; Hu, X.M.; Huang, L.Z. Phosphorus and nitrogen recovery from wastewater by ceramsite: Adsorption mechanism, plant cultivation and sustainability analysis. *Sci. Total Environ.* **2022**, *805*, 150288. [[CrossRef](#)]
31. Viraraghavan, T.; De Maria Alfaro, F. Adsorption of phenol from wastewater by peat, fly ash and bentonite. *J. Hazard Mater.* **1998**, *57*, 59–70. [[CrossRef](#)]
32. Binner, I.; Dultz, S.; Schellhorn, M.; Schenk, M.K. Potassium adsorption and release properties of clays in peat-based horticultural substrates for increasing the cultivation safety of plants. *Appl. Clay Sci.* **2017**, *145*, 28–36. [[CrossRef](#)]
33. Zhu, W.L.; Cui, L.H.; Ouyang, Y.; Lon, C.F.; Tang, X.D. Kinetic Adsorption of Ammonium Nitrogen by Substrate Materials for Constructed Wetlands. *Pedosphere* **2011**, *21*, 454–463. [[CrossRef](#)]
34. Brião, G.V.; Da Silva, M.G.C.; Vieira, M.G.A. Dysprosium adsorption on expanded vermiculite: Kinetics, selectivity and desorption. *Colloid Surface A* **2021**, *630*, 127616. [[CrossRef](#)]
35. Panuccio, M.R.; Sorgonà, A.; Rizzo, M.; Cacco, G. Cadmium adsorption on vermiculite, zeolite and pumice: Batch experimental studies. *J. Environ. Manag.* **2009**, *90*, 364–374. [[CrossRef](#)] [[PubMed](#)]
36. Malamis, S.; Katsou, E. A review on zinc and nickel adsorption on natural and modified zeolite, bentonite and vermiculite: Examination of process parameters, kinetics and isotherms. *J. Hazard Mater.* **2013**, *252*, 428–461. [[CrossRef](#)]
37. Jiang, F.Y.; Qi, Y.L.; Shi, X.S. Effect of Liquid Carbon Sources on Nitrate Removal, Characteristics of Soluble Microbial Products and Microbial Community in Denitrification Biofilters. *J. Clean. Prod.* **2022**, *339*, 130776. [[CrossRef](#)]
38. Guo, F.C.; Xu, F.; Cai, R.; Li, D.X.; Xu, Q.Y.; Yang, X.Y.; Wu, Z.S.; Wu, Y.B.; Wang, Q.H.; Ao, L.G.; et al. Enhancement of Denitrification in Biofilters by Immobilized Biochar under Low-temperature Stress. *Bioresour. Technol.* **2022**, *347*, 126664. [[CrossRef](#)]
39. Zhou, Y.; Chen, F.X.; Chen, N.; Peng, T.; Dong, S.S.; Feng, C.P. Denitrification Performance and Mechanism of Biofilter Constructed with Sulfur Autotrophic Denitrification Composite Filler in Engineering Application. *Bioresour. Technol.* **2021**, *340*, 125699. [[CrossRef](#)]
40. Lu, W.K.; Zhang, Y.L.; Wang, Q.Q.; Wei, Y.; Bu, Y.A.; Ma, B. Achieving Advanced Nitrogen Removal in a Novel Partial Denitrification/anammox-nitrifying (PDA-N) Biofilter Process Treating Low C/N Ratio Municipal Wastewater. *Bioresour. Technol.* **2021**, *340*, 125661. [[CrossRef](#)]
41. Cui, B.; Yang, Q.; Liu, X.H.; Wu, W.J.; Liu, Z.B.; Gu, P.C. Achieving Partial Denitrification-anammox in Biofilter for Advanced Wastewater Treatment. *Environ. Int.* **2020**, *138*, 105612. [[CrossRef](#)] [[PubMed](#)]
42. Wang, Y.; Li, B.J.; Xue, F.R.; Wang, W.H.; Huang, X.Z.; Wang, Z. Partial Nitrification Coupled with Denitrification and Anammox to Treat Landfill Leachate in a Tower Biofilter Reactor (TBFR). *J. Water Process Eng.* **2021**, *42*, 102155. [[CrossRef](#)]
43. Gao, Y.L.; Huang, H.; Peng, C.; Fan, X.; Hu, J.; Ren, H.Q. Simultaneous Nitrogen Removal and Toxicity Reduction of Synthetic Municipal Wastewater by Micro-electrolysis and Sulfur-based Denitrification Biofilter. *Bioresour. Technol.* **2020**, *316*, 123924. [[CrossRef](#)] [[PubMed](#)]
44. Zhou, Q.; Sun, H.M.; Jia, L.X.; Wu, W.Z. Simultaneously advanced removal of nitrogen and phosphorus in a biofilter packed with ZVI/PHBV/sawdust composite: Deciphering the succession of dominant bacteria and keystone species. *Bioresour. Technol.* **2022**, *347*, 126724. [[CrossRef](#)] [[PubMed](#)]
45. Lin, Z.Y.; Wang, Y.M.; Huang, W.; Wang, J.L.; Chen, L.; Zhou, J.; He, Q. Single-stage denitrifying phosphorus removal biofilter utilizing intracellular carbon source for advanced nutrient removal and phosphorus recovery. *Bioresour. Technol.* **2019**, *277*, 27–36. [[CrossRef](#)] [[PubMed](#)]
46. Zhou, Z.J.; Xu, P.; Cao, X.Y.; Zhou, Y.Y.; Song, C.L. Efficiency promotion and its mechanisms of simultaneous nitrogen and phosphorus removal in stormwater biofilters. *Bioresour. Technol.* **2016**, *218*, 842–849. [[CrossRef](#)]